

# SELECTION OF UNRESOLVED HYPERFINE STATES IN ATOMS AND MOLECULES VIA AUTLER-TOWNES EFFECT

T. Kirova<sup>1</sup>, A. Ekers<sup>1</sup>, M. Auzinsh<sup>1</sup>, N. Bezuglov<sup>2</sup>, K. Blushs<sup>1</sup>

<sup>1</sup> Institute of Atomic Physics and Spectroscopy, University of Latvia, Riga, Latvia

<sup>2</sup> Fock Institute of Physics, St. Petersburg State University, St. Petersburg, Russia

*Autler-Townes effect is studied in atomic and molecular level systems where hyperfine structure is present. A three-level ladder scheme coupled by two laser fields is investigated in Na and Na<sub>2</sub> by using a theoretical model based on solving the density matrix equations of motion. Simulations show that application of a strong coupling field between the intermediate and the final states of the ladder results in resolution of the  $M_F$  Zeeman sublevels of the hyperfine levels  $F$  if the hyperfine structure is resolved. This resolution vanishes if the hyperfine levels are initially unresolved spectroscopically. In Na<sub>2</sub>  $M_F$  components can be resolved if the excitation spectra are calculated separately for selected sub-ladders of  $F$ -levels. Inclusion of all  $F$ -levels simultaneously leads to disappearance of the HFS from the excitation spectra. Future work should clarify the possibility to use the dressed-state approach to selectively address HFS levels which are initially unresolved.*

## Introduction

The Autler-Townes (AT) effect [1] is the high-frequency analogue of the splitting of two degenerate levels by a dc Stark field. It has a potential for development of new applications to molecular spectroscopy, like obtaining the transition dipole moment matrix element [2- 3] as well as lifetime and branching ratios of highly excited molecular states using cw laser fields [4]. The possibility to achieve quantum state control using the AT effect has been studied by using the Nonresonant Dynamic Stark Effect (NRDSE) [5] and the Selective Population of Dressed States (SPODS) [6] techniques. An all-optical method for aligning non-polar molecules for chemical reactions was demonstrated [3] based on the AT effect and its dependence on the molecular magnetic quantum number ( $M_J$ ). The latter enables resolution of individual  $M_J$  peaks, leading to additional state selectivity and better control of the molecular properties. In our present work we extend the quantum control schemes to more complex energy level systems. In particular, the effect of coupling between nuclear and electronic angular momentum, which leads to occurrence of hyperfine structure, is studied in atomic and molecular level systems. Each atomic/molecular hyperfine level  $F$  is  $2F+1$ -fold degenerate over the projection of  $F$  (i.e.,  $M_F$ ). Since the coupling of hyperfine components by the laser field depends on the hyperfine and magnetic quantum numbers, this will lead to a different AT splitting for each involved hyperfine level and thus to resolution of the  $F$  and  $M_F$  components.

## Results

We consider a specific application of a three-level ladder scheme in Na, as shown in Fig. 1. A weak probe laser P excites the atoms from the ground state  $|g\rangle$  ( $3S_{1/2}$ ,  $F_g=1, 2$ ) to the intermediate state  $|e\rangle$  ( $3P_{1/2}$  state,  $F_e=1, 2$ ), which is further coupled by a strong laser field S to the final state  $|f\rangle$  ( $5S_{1/2}$ ,  $F_f=1, 2$ ). The transition dipole matrix element between two hyperfine states can be then evaluated as [7]

$$\langle F_f M_{F_f} | \mu_q | F_e M_{F_e} \rangle = (-1)^{F_f - M_{F_f}} \begin{pmatrix} F_f & 1 & F_e \\ -M_{F_f} & q & M_{F_e} \end{pmatrix} \quad (1)$$

$$(-1)^{F_f + I + J_e + 1} \sqrt{(2F_e + 1)(2F_f + 1)} \begin{Bmatrix} J_e & F_e & I \\ F_f & J_f & 1 \end{Bmatrix} (J_f \| \mu \| J_e),$$

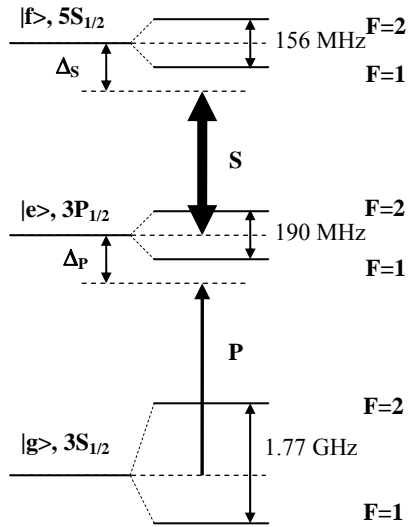


**Fig.1.** Excitation Scheme in Na.

The total Hamiltonian of the system can be written as

$$\hat{H} = \hat{H}_0 + \hat{V}, \quad (3)$$

with  $\hat{H}_0$  being the unperturbed atomic/molecular Hamiltonian and  $\hat{V} = -\hat{\mu} \cdot \vec{E}$  representing the dipole interaction operator. The optical Bloch equations (OBEs) for the density matrix are then given by

$$\frac{d\rho}{dt} = -\frac{i}{\hbar} [\hat{H}, \rho] + \hat{R}\rho, \quad (4)$$

where  $\hat{R}$  accounts for relaxation due to spontaneous emission as well as transit relaxation of the atoms through the laser beam. Equation (4) gives the OBEs for Zeeman coherences  $\rho_{g_i, g_j}, \rho_{e_i, e_j}, \rho_{f_i, f_j}$  and optical coherences  $\rho_{g_i, e_j}, \rho_{e_i, g_j}, \rho_{e_i, f_j}, \rho_{f_i, e_j}$ , after solving of which the fluorescence spectra of levels  $|g\rangle$ ,  $|e\rangle$ , and  $|f\rangle$  can be calculated. For a full description of the model used here see reference [8].

Using the theoretical model described above we perform numerical simulations for the population of level  $|f\rangle$  including the interaction of both laser fields with all the hyperfine levels in the system. In view of planned future experiments in atomic/molecular beams, the Doppler broadening is not accounted for.

Figure 2 shows the final state population as a function of the probe laser detuning for four different values of the coupling field Rabi frequency. At low intensity of the coupling laser S, the fluorescence signal consists of two pairs of peaks corresponding to the excitation from the two hyperfine components of level  $|g\rangle$  to the two hyperfine components of level  $|f\rangle$ . As the coupling field Rabi frequency increases, a separation of Zeeman sublevels  $M_F$  is seen until their full resolution at  $\Omega_S = 1000$  MHz. Note that the strong field coupling Rabi frequency in the latter case exceeds by several times the hyperfine splittings of both the  $3P_{1/2}$  state ( $\Delta E_{F=1, F=2} = 188.88$  MHz) and the  $5S_{1/2}$  state ( $\Delta E_{F=1, F=2} = 156$  MHz). The laser linewidths of both laser fields are taken to be 1 MHz.

Next, we investigated the effect of the hyperfine constant, and therefore splitting between the hyperfine levels, on the resolution of the magnetic sublevels upon interaction with strong coupling field. As seen in Fig. 3, the reduction of the hyperfine constant  $A_{\text{hfs}}$  of the final state by a factor of two and ten, leads to inability to resolve the  $M_F$  sublevels.

Finally, the application of a strong laser field was studied in a similar excitation scheme in  $\text{Na}_2$ , where state  $|g\rangle$  is the  $X^1\Sigma_g^+$  ( $J=1$ ) state, state  $|e\rangle$  is the  $A^1\Sigma_u^+$  ( $J=0$ ) state and

after applying the Wigner-Eckert theorem and taking into account that  $\mathbf{F} = \mathbf{I} + \mathbf{J}$  ( $\mathbf{I}$  is the total nuclear spin and  $\mathbf{J}$  the total electron angular momentum). Here,  $(J_f \| \mu \| J_e)$  is the reduced matrix element, and the expressions in  $()$  and  $\{\}$  brackets represent the 3j and 6j symbols, respectively. Since the Rabi frequency of the strong coupling field is defined as

$$\Omega_S = \frac{\langle F_f M_{F_f} | \mu_q | F_e M_{F_e} \rangle E_S}{\hbar}, \quad (2)$$

the  $F$  and  $M_F$  dependence given by Eq. (1) transfers to Eq. (2), and consequently to the associated with it splitting of the AT doublet. Therefore, we can use the above expressions to find the energy positions of each hyperfine and magnetic sublevel components, which give rise to the AT peaks in the fluorescence spectra of levels  $|e\rangle$  and  $|f\rangle$ .

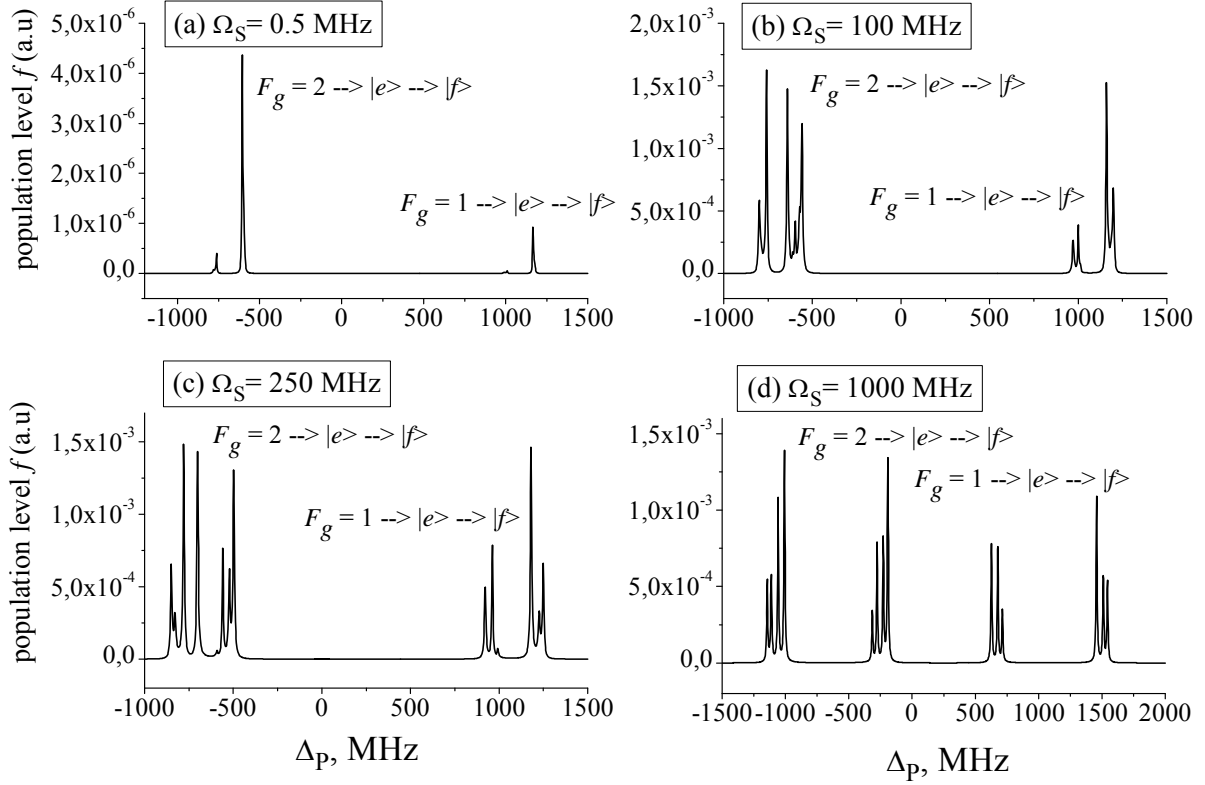


**Fig. 2.** Population of level  $|f\rangle$  vs probe field detuning for different S field Rabi frequencies. Simulations are performed using parameters  $\Omega_p=0.5$  MHz, transit relaxation of 1 MHz, laser linewidth of 1 MHz for both laser fields, and lifetimes of the  $3P_{1/2}$  and  $5S_{1/2}$  states of 16.35 ns and 77.6 ns, respectively.

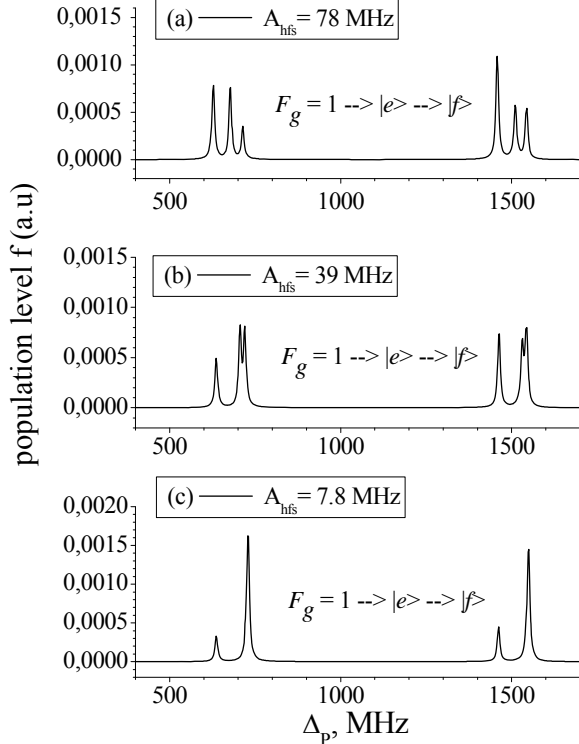


**Fig.3.** The  $F_g=1 \rightarrow |e\rangle \rightarrow |f\rangle$  component of the excitation spectrum in Fig. 2d for different values of  $A_{\text{hfs}}$ . All other simulation parameters are equal to those used for Fig. 2.

$5^1\Sigma_g^+(J=1)$  represents the final state  $|f\rangle$ . In this case the hyperfine splittings are of an order of  $10^{-1} \div 10^2$  kHz which is well below the natural widths of levels  $|e\rangle$  and  $|f\rangle$ . Figures 4a-c show the full resolution of the magnetic sublevels  $M_F$  by using a coupling field of Rabi frequency  $\Omega_s=250$  MHz when only one hyperfine level  $F_f$  in the final state is considered. However, the inclusion of more than one hyperfine level in the final state leads to a complete loss of the  $M_F$  resolution (Fig.4d). Similar results are also obtained in the case of narrow laser linewidth (1 Hz) or long lived final state (lifetime of 100  $\mu$ s).

### Discussion

Our simulations based on solving the OBEs for the density matrix showed that the use of strong enough laser field can lead to full lifting of the  $M_F$  degeneracy, which gives the opportunity

to selectively address magnetic sublevels in excited atomic and molecular states. The latter is, however, only true when hyperfine structure can be initially resolved by the usual spectroscopic means. This could be intuitively anticipated remembering that no hyperfine structure associated effects are resolved in atomic spectroscopy experiments in the limit of broad spectral line [9]. Further work is in progress to understand the above effects in the case of unresolved hyperfine structure and to understand the limits of application of the theoretical model and to predict possible experimental applications. This work is expected to result in novel approaches allowing one to achieve selective addressing of initially unresolved hyperfine states using cw lasers in double-resonance experiments.

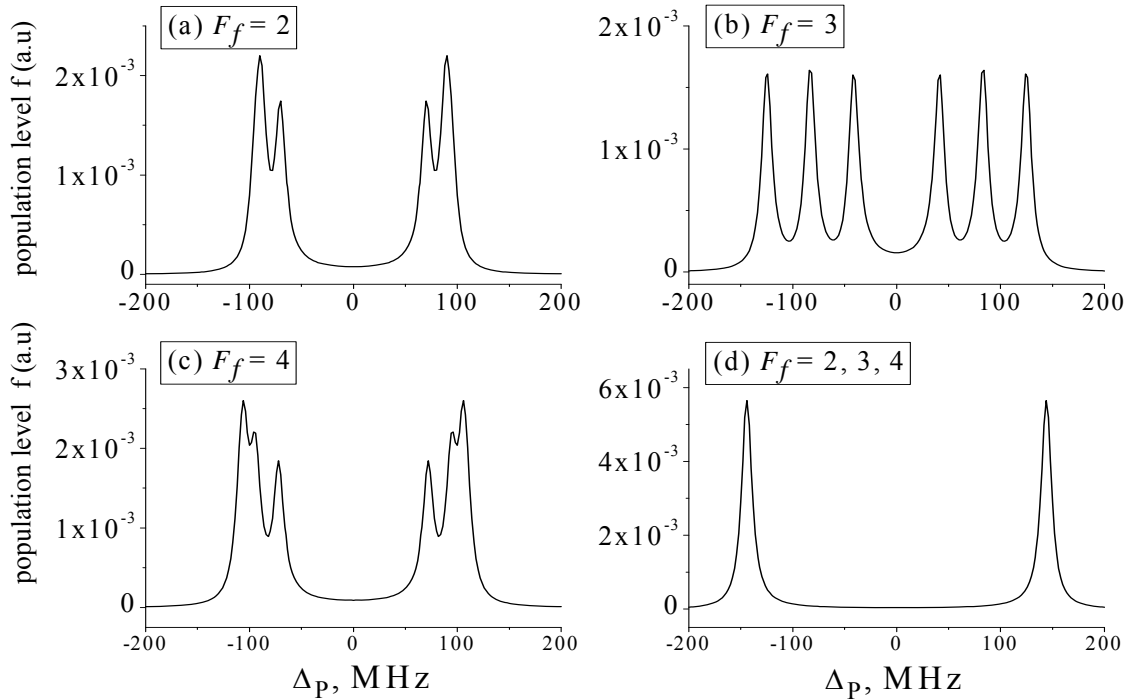


**Fig. 4.** Population of level  $|f\rangle$  vs probe field detuning calculated for each hyperfine component separately (frames (a), (b), and (c)) and for all components simultaneously (frame (d)). The simulations were performed with  $\Omega_S=250$  MHz,  $\Omega_p=0.5$  MHz, transit relaxation of 1 MHz, linewidths of both laser fields of 1 MHz, and lifetimes of the  $A^1\Sigma_u^+$  and  $5^1\Sigma_g^+$  states of 12.45 ns and 40 ns, respectively.

This work was supported by the EU FP6 TOK project LAMOL, NATO grant EAP.RIG.981378, European Social Fund, and Latvian Science Council.

## REFERENCES

- [1] S. H. Autler and C. H. Townes, Phys. Rev. **100**, 703 (1955)
- [2] M. A. Quesada et al., Phys. Rev. A, **36**, 4107 (1987); J. Qi et al., Phys. Rev. Lett., **88**, 173003 (2002);
- [3] J. Qi et al., Phys. Rev. Lett., **83**, 288 (1999)
- [4] R. Garcia-Fernandez et al., Phys. Rev. A, **71**, 023401 (2005)
- [5] B. J. Sussman et al., PRA **71**, 051401 (2005); PRA **73**, 053403 (2006)
- [6] M. Wollenhaupt et al., J. Opt. B **7**, S270 (2005); M. Wollenhaupt et al., Chem. Phys. Lett. **419**, 184 (2005); M. Wollenhaupt et al., PRA **73**, 063409 (2006)
- [7] R. N. Zare, *Angular Momentum*, Wiley-Interscience, New York, 1986
- [8] M. Auzinsh et al, Opt. Commun. **264**, 333 (2006)
- [9] W. Happer, Reviews of Modern Physics. **44**, 169 (1972)